Source area and rupture parameters of the 31 December 1881 M_w = 7.9 Car Nicobar earthquake estimated from tsunamis recorded in the Bay of Bengal

Modesto Ortiz

Departamento de Oceanografía, Centro de Investigación Cientifica y Educación Superior de Ensenada, Ensenada, Baja California, Mexico

Roger Bilham

Cooperative Institute for Research in Environmental Sciences and Department of Geological Sciences, University of Colorado, Boulder, Colorado, USA

Received 24 April 2002; revised 14 November 2002; accepted 23 January 2003; published 23 April 2003.

[1] On the morning of 31 December 1881 a submarine earthquake beneath the Andaman Islands generated a tsunami with a maximum crest height of 0.8 m that was recorded by eight tide gauges surrounding the Bay of Bengal. Since the earthquake occurred 8 years before the construction of the world's first teleseismic recording seismometer, little has been known about its rupture parameters or location. Waveform and amplitude modeling of the tsunami indicate that it was generated by a $M_w = 7.9 \pm 0.1$ rupture on the India/Andaman plate boundary resulting in 10–60 cm of uplift of the island of Car Nicobar. The rupture consisted of two segments: the northern 40-km-long segment is separated from the southern 150-km-long segment by a 100-km region corresponding to the westward projection of the West Andaman spreading center. The main rupture occurred between 8.5°N and 10°N with a total area of 150 km $\times$ 60 km dipping 20°E with a mean slip of 2.7 m. The recurrence time for 1881-type events is estimated to be 114–200 years on the basis of inferred GPS convergence rates and inferred plate closure vectors, although slip partitioning in the region may extend this estimate by as much as 30%. *INDEX TERMS:* 3025 Marine Geology and Geophysics: Marine seismics (0935); 7215 Seismology: Earthquake parameters; 4564 Oceanography: Physical: Tsunamis and storm surges; 7294 Seismology: Instruments and techniques; 9340 Information Related to Geographic Region: Indian Ocean; *KEYWORDS:* earthquake, rupture zone, tsunami records 1881, Bay of Bengal

Citation: Ortiz, M., and R. Bilham, Source area and rupture parameters of the 31 December 1881 M_w = 7.9 Car Nicobar earthquake estimated from tsunamis recorded in the Bay of Bengal, *J. Geophys. Res.*, *108*(B4), 2215, doi:10.1029/2002JB001941, 2003.

1. Introduction: The 1881 Earthquake

[2] At approximately 0149 UT (0749 LT) on the last day of 1881 a damaging earthquake that occurred near the Andaman Islands was felt over much of India and parts of Burma, and by ships in the Bay of Bengal [*Oldham*, 1884]. The felt area (Figure 1) embraced a region of more than 5×10^6 km^2, similar to $M \geq 8$ earthquakes that were felt in India during the following several decades. Yet damage in the Andaman Islands during the earthquake was relatively modest: masonry barracks and a shoreline dam near Port Blair required repairs, and a brick factory chimney was damaged at its base and required replacement [*Government Report*, 1882]. The tsunami surge at Car Nicobar did not exceed 75 cm since pile floors constructed at greater sea level heights remained dry. Huts were damaged by the shaking. Inland coconut trees on Car Nicobar Island toppled but shoreline trees remained standing [*Rogers*, 1883], and sand venting was reported on the island [*Oldham*, 1884]. Three large aftershocks were reported on 1 Jan 1882 by people on the Nicobar Islands, and also by the ship *Commonwealth* steaming near Car Nicobar (8.3°N, 92.7°E). Numerous aftershocks were reported from Port Blair. Acheen in northern Sumatra reported "severe" shaking, but in India the shaking was gentle, although sufficient for it to have stopped a clock in Madras and to be noticed by people at several points along the coast (see Appendix A).

[3] The population of the Andaman and Nicobar Islands in 1881 consisted largely of a convict colony with 5000 convicts and administrators and an indigenous population scattered throughout the islands whose numbers may have exceeded several thousand. The current population of the Andaman and Nicobar islands is ~360,000 of which 30% live in Port Blair.

[4] The tsunami that was generated by the earthquake propagated throughout the Bay of Bengal and was recorded with amplitudes of a few cm to 1.2 m peak-to-peak [*Oldham*, 1884] by 8 tide gauges whose operation had been initiated a few years earlier by the Survey of India. Tide

0148-0227/03/2002JB001941$09.00

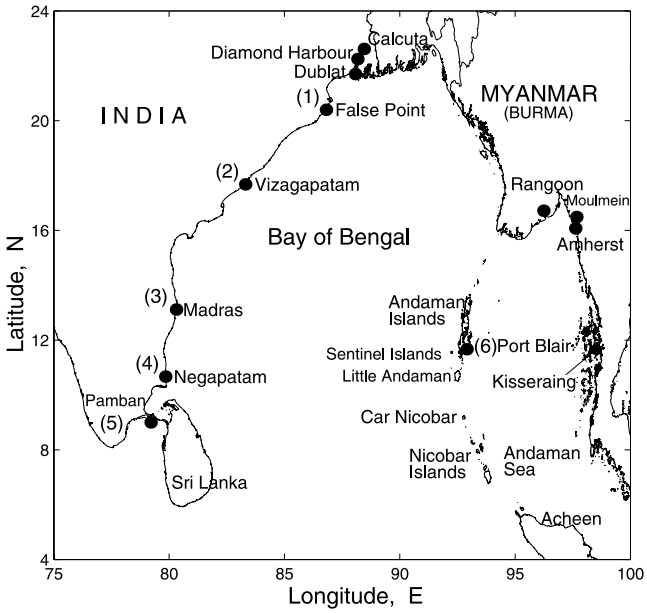

Figure 1. Felt area of the 31 December 1881 Nicobar earthquake. Tide gauges that were in operation at the time of the earthquake are indicated by solid dots. Tide gauges that recorded the tsunami are indicated by numerals 1 to 6. Names refer to the names of Indian cities in 1881.

gauges in operation in the Irrawady delta (Rangoon, Moulmein and Amherst) did not show evidence of any sea wave [*Walker*, 1883].

[5] The article is laid out as follows: in sections 2 and 3 we describe the tectonic setting of the region and the distribution of tide gauges around the Bay of Bengal. In section 4 we examine evidence for the time of the earthquake based on clocks and the availability of seismic wave arrival times recorded on two of the tide gauges and the timing of tsunami waves recorded by six gauges. We then use the timing of tsunami waves recorded by six gauges to obtain an approximate location for the rupture zone by back-propagating oceanic gravity waves to their source using the bathymetry of the Bay of Bengal to determine precise wave paths and velocities. Having identified the approximate location of the 1881 source zone, we invert the closest tsunami at Port Blair to determine the most likely depth, dip, slip, and submarine rupture area for the 1881 earthquake. Finally, we place the inferred rupture zone in its structural setting and estimate a possible recurrence time for similar event using GPS data from Port Blair and Bangalore. Appendix A lists changes of names of Indian cities since 1881 and reproduces original reports of the tsunami.

2. Tectonics of the Region

[6] The Andaman and Nicobar Islands parallel the arcuate plate boundary separating the Indian and Sunda Plates east of the 90°E ridge [*Fitch*, 1970; *Eguchi et al.*, 1979; *Curray et al.*, 1979, 1982; *Banghar*, 1987; *Dasgupta and Mukhopadhyaya*, 1993; *Maung*, 1987; *Rajendran and Gupta*, 1989]. The ridge material is believed to have been formed from sediments scraped off the descending Indian Plate interleaved with ophiolites from the ocean floor beneath the Bengal Fan. In that the islands are bounded to the east by strike-slip faults and spreading centers, and to the west by a subduction zone, the Andaman/Nicobar ridge acts as a small tectonic plate that has been referred to as the Burma Plate by *Curray et al.* [1982] and as the Andaman Plate by *Dasgupta* [1993]. The geology of the Andamans is described by *Oldham* [1885] and *Tipper* [1911]. The schematic tectonics of the region is illustrated in Figure 2.

[7] Global plate reconstructions indicate that at latitude 9°N the Indian Plate converges at N23°E obliquely toward the Asian plate at 54 mm/yr [*DeMets et al.*, 1990, 1994]. This velocity is weakly constrained by these circuit closures, and direct observations of the current Indo-Asian convergence rate indicate that a lower rate may be appropriate [*Wang et al.*, 2001]. Magnetic lineations in the Andaman Sea indicate a mean full spreading rate for the Andaman back arc basin in about the past 4 Myr of ~30 mm/yr, with an inferred azimuth of spreading of 340°, based on the strike of contiguous transform faults (J. Curray, personal communication, 2002). Recent GPS observations between Bangalore and Port Blair indicate that Port Blair approaches the mainland at a rate of 15.3 ± 3 mm/yr at 250° ± 5° which represents a minimum estimate of the India/Andaman plate convergence velocity [*Paul et al.*, 2001] assuming no internal deformation of the Indian Plate.

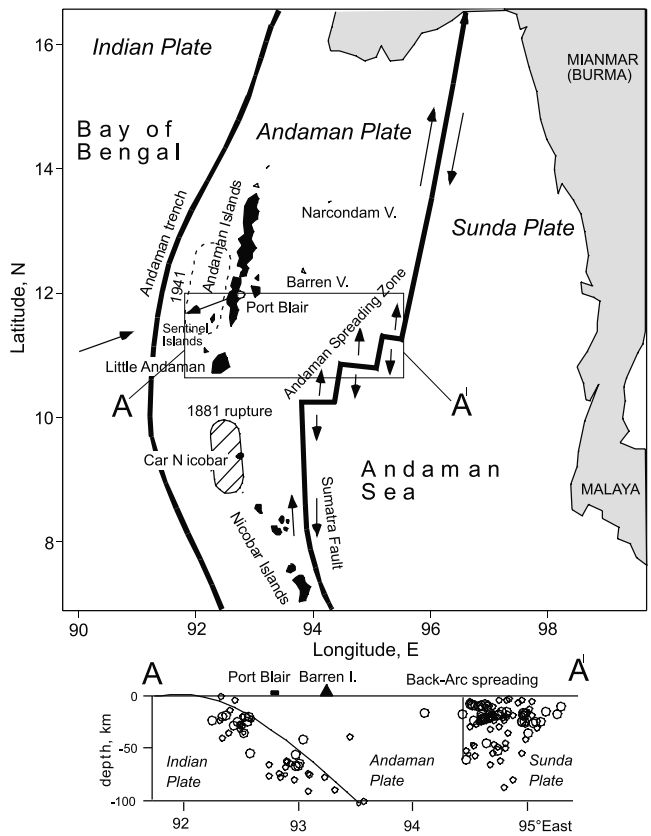

Figure 2. Schematic tectonics near the Andaman and Nicobar Islands. The location of the 1941 earthquake is conjectural. We show the calculated location of the 1881 main rupture near Car Nicobar. Seismicity between 10.8°N and 12°N from *Engdahl et al.* [1998].

[8] The 10°N channel that separates the Andaman and Nicobar Islands shows imbricate thrust sheets dipping gently to the east, parallel to the subduction zone (J. Curray, personal communication, 2001). These faults and associated folding of seafloor sediments may be traced long distances north-south and their recent activity may be responsible for the elevation of carbonate platforms (raised beaches) in Car Nicobar [*Kurz*, 1868] and in the Sentinel islands [*Tipper*, 1911]. Geomorphic evidence (drowned forests) suggests that the Andaman Islands are tilting down to the east [*Oldham*, 1884; *Tipper*, 1911].

[9] Near the Nicobar Islands (8–10°N) strike-slip faulting is manifest on the Sumatra Fault, a prominent northward continuation of the Sunda Fault. North of approximately 10.2°N the active transform is offset ~100 km to the east by the Andaman spreading center, and the Sumatra Fault is represented by an inactive fracture zone. North of this latitude the Burma Plate broadens and the partitioning of strike-slip and thrust components are widely separated. It is perhaps for this reason that the Benioff zone is clearly expressed by microseismicity north of 10°N and less clearly to the south. Cross sections of well-located microseismicity in the region since 1964 [*Engdahl et al.*, 1998] show the Indian Plate to dip east 15–40° between 7°N and 12°N.

[10] The historical record of earthquakes in the Andaman and Nicobar islands is poor because the indigenous population kept no records, and because colonial occupation was patchy prior to the mid-nineteenth century. Jesuits visited the Nicobar Islands in 1711, and a Danish colony was established 1759–1773 which encouraged Moravian settlement in the interval 1768–1787. A brief occupation of the Nicobars by Austrians 1778–1781, led to the return of a Danish garrison 1784–1837, interrupted by British occupation during the Napoleonic wars 1807–1814, and followed by British administration (1869–1945). In the Nicobar Islands' Gazetteer, earthquakes "of great violence are recorded in 1847 (31 October to 5 December), 1881 with tidal wave (31 December), and milder shocks in 1899 (December)". A sequence of great earthquakes in 1883 and 1861 in Sumatra progressively approached the region of the 1881 earthquake [*Newcomb and McCann*, 1987].

[11] The Andaman Islands to the north of the Nicobars were occupied by colonial powers somewhat later. A British government report [*Home Department*, 1859] that claims to compile "nearly, if not quite, all that is known regarding the Andaman Islands" omits all mention of earthquakes in the period 1774–1850, (the time of the first survey of the islands) presumably because continuous occupation of the islands was initiated only after the establishment of a penal colony in 1858. The Imperial Gazetteer [*Hunter et al.*, 1909] repeats entries from the Andaman Gazetteer in listing several events without attribution "minor earthquakes occurred in August 1868; February 1880; and then shocks at intervals till December 31st, 1881; February 1882; August 1883; July 1894; October, 1899".

[12] The most recent great earthquake (M_s = 8.1, 26 June 1941) to rupture the Andaman Plate Boundary [*Krishnan*, 1953; *Jhingran*, 1953; *Sinvhal et al.*, 1978; *Srivastava and Chaudhury*, 1979] occurred during a brief occupation of the islands by the Japanese in World War II, when the reporting and recording of natural phenomena assumed a low priority, and in some cases were deliberately suppressed. The tsunami generated by the 1941 earthquake is stated to have caused much loss of life along the east coast of India [*Murty and Rafiq*, 1991], although we have been unable to confirm this. Part of the cellular jail, a large masonry structure near Port Blair, collapsed along with other masonry structures. Slumping, liquefaction and sand venting were recorded by eyewitnesses. Islands in the passage between Little Andaman and South Andaman sank >50 cm based on shoreline submergence and by >1.5 m based on seafloor soundings. Thirty-nine reports of intensities were estimated to not exceed Mercalli intensity VIII on most of the Andamans, with slightly higher intensity near Port Anson on the SW coast on Middle Andaman. Aftershocks were felt with diminishing frequency for the following 3 months [*Jhingran*, 1953]. A damaging earthquake with a strike-slip mechanism (M = 6.2) caused damage in the Nicobar Islands in 1982 [*Agrawal*, 1983].

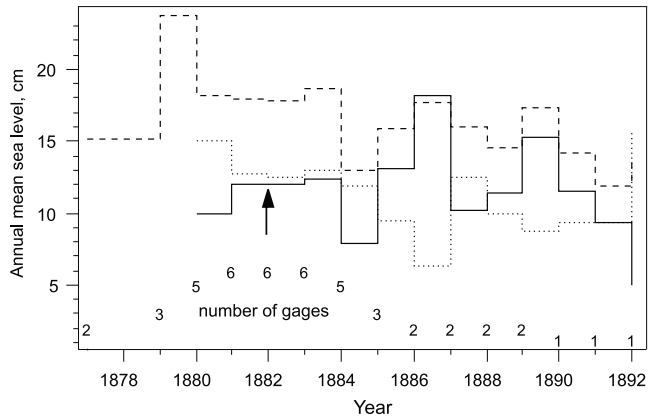

Figure 3. Annual mean sea level for the northern Indian Ocean 1878–1892. Dashed line is the mean of tide gages around the Bay of Bengal, including Bombay but excluding Port Blair (number of operating gages indicated below). The dotted trace is the Port Blair annual mean, and the solid trace is the difference between the Port Blair record and mean sea level (plotted as harbor uplift upward). The arrow indicates the time of the 1881 earthquake. The 1881–1883 period is distinguished by its low variance in Bay of Bengal sea level, and by the absence of evidence for vertical uplift or subsidence at Port Blair.

3. Bay of Bengal Tide Gauges

[13] More than a dozen tide gauges were established in the Indian Ocean Ports by the Great Trigonometrical Survey of India in the late 1870s to determine tidal harmonics for the prediction of harbor tide tables and to provide datums for the correction of propagating errors in spirit-leveling operations [*Eccles*, 1901]. In many cases the tide gauges were operated for no more than a few years and removed when sufficient data had been collected. It is thus serendipitous that the largest deployment of operating gauges (see Figure 3) should coincide with the occurrence of both the 1881 earthquake and the 1883 Krakatau eruption, for which good tsunami records were obtained.

[14] The gauges consisted of a heavy vertical standpipe (a stilling well), usually 56 cm in diameter and up to 6 m long, embedded in the seafloor and connected hydraulically

Table 1. Tide Gauge Specifications and Time of First Arrival Waves Around the Bay of Bengal[a]

Location	Coordinates	Pipe Diameter		Length, m	τ, s	Scale	Seismic Wave, h:m:s	Tsunami Wave (clock), LT	ObsT-s Delay, min	Maximum Amplitude, m
		Stand, m	Inlet, mm							
Calcutta	22.55°N, 88.3°E						7:55:02			. . .
Diamond Hbr	22.18°N, 88.18°E							1510	441[b]	<0.02
Dublat	21.5°N, 88°E							1300	311[b]	<0.02
False Point	20.42°N, 86.78°E	1.22	50.8	3.66	43	0.3	7:54	1115	201-8	0.03
Kisseraing	11.65°N; 98.52°E						(7:55)	(clock)		<0.01
Madras	13.11°N; 80.30°E	0.18	3	0.005	100	1	7:55:36	1020	144[b]	0.25
Moulmein	16.48°N;97.62°E	0.69	pinhole	. . .	. . .	0.25		none		none
Negapatam	10.67°N; 79.83°E	0.69	pinhole	. . .	. . .	1	. . .	1015	145[b]	0.80
Pamban	9.16°N; 79.2°E	0.56	50.8	24.7	60.4	1	. . .	1132	223[b]	0.25
Port Blair	11.67°N; 92.75°E	0.56	69.85	18.3	12.5	0.5	7:44	0803	19–21	0.90
Vizagapatam	17.68°N; 83.28°E	0.56	50.8	9.14	22.4	0.5	. . .	1043	174[b]	0.15

[a]Times indicated are Port Blair time, which at 90°E is 6 hours in advance of UT. The stilling well (standpipe) diameter and inlet pipe diameter and lengths of the tide gauges are used to calculate time constants, τ. A scale of 1 indicates that sea level is recorded directly on the chart without amplification. Tsunami-seismic (T-s) wave travel times are listed for observed tsunamis in hours:minutes:seconds (h:m:s). The T-s delay entered for False Point and Port Blair includes the uncertainty caused by whether the body or surface waves were registered by the tide gauges.

[b]Times are estimated from an inferred 0749 main shock time (see text).

to the sea via a siphon pipe, or where this was found to be difficult to maintain, by a set of holes. In some cases a long wooden box was constructed from teak (e.g., Negapatam) instead of using a cylindrical metal pipe. A float connected to a counterbalance weight via a pulley rotated a horizontal drum via a reduction gear, whereby the movement of the perimeter of the drum represented some fraction of the motion of the float. A pen driven along the top of the drum by a clockwork mechanism recorded continuously the position of the float. A new paper chart was wrapped around the drum each week on which to record the tidal motions and in some locations the presence of seiches.

[15] Each tide gauge was inspected four times each day to verify operation (twice only on Sundays). Records were maintained of the synchronization of the chart relative to Madras time at 4 p.m. each day to an accuracy of a few seconds using telegraphic time transfer, supplemented by a portable watch provided to the operator specifically to carry the time from the telegraphic office to the tide gauge. The clock that drove the drum was adjusted only when the clock error exceeded 30 s.

[16] Short period wave motion was filtered hydraulically by the incorporation of a small diameter inlet to the sea. The time constant of the geometries used in the Indian tide gauges can be calculated from an expression of the form $\tau = 8\nu La^2/(r^4 g)$, where a and r are the radii of the stilling well and inlet pipes respectively, L is the length of the inlet pipe, and $\nu = 0.01$ cm^2/s is the kinematic viscosity of seawater [*Bilham*, 1977]. Time constants varied from 12.5 s at Port Blair to perhaps 100 s at Madras. The time constant for the Madras gauge and others that used perforations instead of pipes to connect to the sea (Pamban and Negapatam) were not possible to evaluate precisely, and clearly changed with time due to fouling of the orifice. The initial time constant of the Madras gauge can be estimated from the dimensions of the single hole in a copper entry pipe described by *Eccles* [1901], but this is likely to be only approximate because of the nonlinearity associated with such systems [*Agnew*, 1986]. The fundamental period of the tsunami at Port Blair, where the most energetic tsunami arrived, is of the order of 20 min with an amplitude of 0.5 m, so that the inferred 12.5 s time constant of the Port Blair gauge attenuates this tsunami wave by <10%.

[17] Because of the difficulty in reading the weekly record if the drum rotated more than one complete revolution during the semidiurnal tide, reduction gearing was used in ports with a large tidal range. With 1:1 gearing, sea level could be recorded to 1 mm precision. With 3:1 gearing (a scale of 0.3 in Table 1), necessary to prevent overlapping data where the tidal range exceeded 2 m, the resolution fell to 3 mm. The copies of these records now available to us (Figure 4) are of lower accuracy because of drafting errors and lower precision (3–15 mm) because of their reduced size when reproduced in subsequent reports. The original data may still exist but attempts to locate them have been unsuccessful.

[18] The zero datum of the chart was linked to a nearby bench mark using spirit leveling methods in order to determine vertical stability of the standpipe and to preserve the long-term datum of the gauge in case of damage by storms, or by port activities, or by changes in the registration of the tide gauge gearing with the sprocket holes on the metal band supporting the float. Hourly values of sea level for each year were analyzed to estimate annual mean sea level to 0.3 mm precision, a value that was then used to provide a sea level datum for the tide gauge bench mark. Mean sea level data for 1879 to 1890 are shown in Figure 3. No significant vertical motion of Port Blair occurred at the time of the earthquake indicating that it was either at a node in the deformation field, or that the earthquake was sufficiently distant to produce no significant deformation at Port Blair.

4. Time of the Main Shock and Travel Time From Seismic and Tsunami Arrivals

[19] There were no seismometers in use at the time of the 1881 earthquake, yet the arrival of seismic waves at False Point and Port Blair were recorded by the continuous tide gauges at these locations, and by observers attending astronomical clocks in Calcutta and Madras. In this section we estimate the absolute time of the earthquake and the

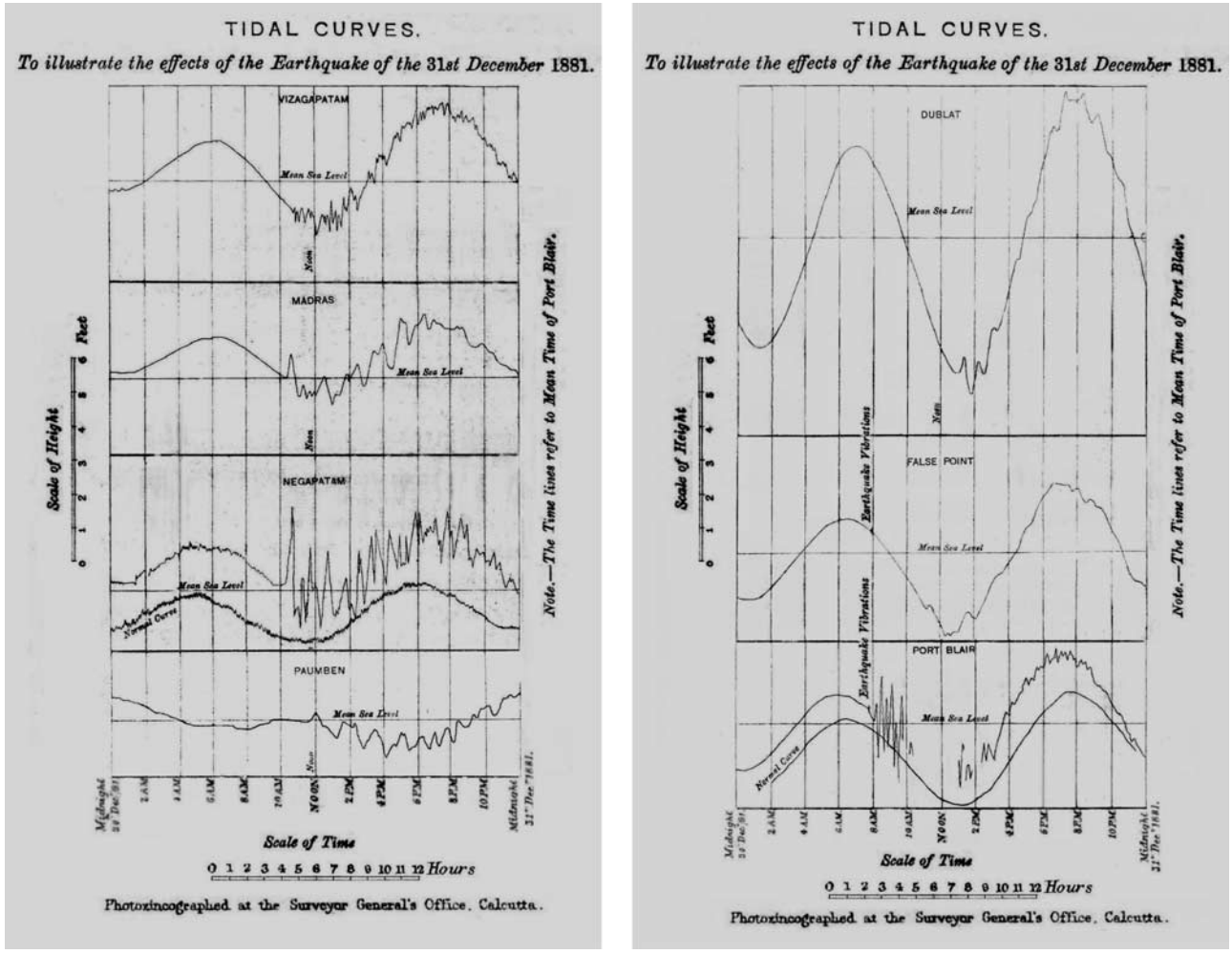

Figure 4. The 31 December 1881 tsunami recorded at Vizagapatam, Madras, Negapatam, Pamban Dublat, False Point, and Port Blair. Vertical lines indicate intervals of 2 hours from Midnight of 30 December to Midnight of 31 December 1881 (Port Blair time). The ''normal curve'' for Negapatam and Port Blair refers to the tide prediction printed by the tide prediction machine. (Figure reproduced from *Oldham* [1884]).

approximate distance from two of the gauges using the tsunami-minus-surface-wave (T-S) travel time.

[20] The tide gauge timing of mainland gauges was synchronized telegraphically by the clock in Madras, but the timing of the Port Blair gauge was set by a chronometer linked to local time and may be associated with an additional error of ±30 s. One other observation of time was made by *Rogers* [1883], who was surveying ~50 km south and 170 km east of Port Blair on the Burmese island of Kisseraing, who notes the time of his theodolite image beginning to undulate at 07:55. *Oldham* [1884] felt this time to be unreliable when he discussed their accuracy with Rogers in 1884, and we follow Oldham in ignoring these data.

[21] We are unable to establish whether the clocks record the times of body waves or (more probably) surface waves, a possible uncertainty of more than 3 min for $\Delta \approx 13°$. Notwithstanding this difficulty, the almost identical arrival times of the seismic wave at Calcutta and Madras (Table 1) were used by Oldham to infer that the earthquake occurred on the locus of these two points, a straight line that intersects the Eurasia/India plate boundary near the Andaman Islands. Because no accurate seismic wave velocities were available at that time, his epicentral distance was too low and was biased by the earlier determination of the epicenter by *Rogers* [1883], repeated by *Walker* [1883, 1884] that suggested an epicentral location of 15°N, 89°E ($\Delta = 9°$), 300 km NW of the plate boundary in the eastern Bengal Fan. We determine a substantially more southeasterly epicentral location in this article.

[22] Oldham corrected the times of arrival of the tsunamis mentioned by *Walker* [1883] and *Rogers* [1883] by inspecting the original tsunami records, and these times are listed in Table 1. The original tsunami records are unavailable for study although reduced copies were published by both Walker and Oldham and are reproduced as Figure 4. Oldham comments that the time resolution of the pencil tide gauge charts was ~30 s. Hence the data from the two tide gauges that recorded both the seismic wave and the tsunami wave record this relative time to an accuracy of ±1 min and by assuming appropriate velocities for the seismic and tsunami waves one can determine an epicentral distance for these tide gauges. We evaluate this first for Port Blair.

[23] The delay between the tsunami and seismic arrivals is estimated as 19–21 min at Port Blair depending on whether body waves or surface waves were registered by the tide gauge. For a surface wave velocity of 3.5 km/s and a tsunami velocity of 0.1 km/s near Port Blair (mean sea depth of 1 km) the epicentral distance is 65 km. It is possible that the tide gauge recorded the body wave arrivals (~5 km/s) on the chart in which case the epicentral distance would have been ~100 km. If one assumes unreasonably shallow (500 m) or significantly deeper (2 km) oceanic paths for a tsunami generated within 200 km of Port Blair the additional tsunami wave uncertainty changes these estimates by <20%. Hence, if the tsunami and seismic waves were generated coincidentally, one can infer that the epicenter of the earthquake lay within a 120-km radius of Port Blair. It is, however, possible that the tsunami was induced by a triggered submarine slump, closer to Port Blair than the main shock, in which case 120 km represents a minimum distance of the main shock from Port Blair. From these data we estimate that the 1881 epicenter lies on a circle at least 120 km in radius from Port Blair.

[24] The False Point tide gauge record also provides an epicentral distance but with less accuracy because the peak-to-peak amplitude of the tsunami was <5 cm and the onset of its arrival is less clear. Oldham's readings indicate a 201-min delay between the seismic wave and tsunami corresponding to an epicentral distance that varies according to the travel path taken by the tsunami, and again depends on whether the seismic body or surface waves were registered by the tide gauge. We compute the tsunami travel time below by integrating the velocity throughout the Bay of Bengal and find that it intersects the inferred Port Blair epicentral circle, 150–200 km south of the Andaman Islands.

[25] From this approximate knowledge of the epicentral location ($\Delta \approx 12.7^\circ$ from both Madras and Calcutta) we estimate from the Jeffreys-Bullen curves that the earthquake occurred 3.3–6.5 min before being recorded by clocks in Calcutta or Madras, depending on whether the gauge registered body wave or surface wave times. Hence the time of the main shock is deduced to have occurred between 0749 and 0752 LT, assuming the same phase was registered by the clocks and tide gauge. From this epicentral time and its uncertainty we may estimate the approximate travel times of tsunamis from the epicentral region to the remaining tide gauges. The onset of the tsunami in each tide gauge record is somewhat emergent. In section 5 we outline details of how the tide gauge records were processed in order to separate the tsunami signal from the ocean tide signal.

5. Removal of the Tide From the Tsunami Record

[26] In general, the travel times of the leading tsunami wave (Table 1) decrease southward along the west coast of the Bay of Bengal, whereas their peak amplitudes decrease northward. Exceptions occur where the tide gauges are deep within river estuaries (e.g., Diamond Harbour, record not showed) or are fronted by wide continental shelf (e.g., Pamban in the Palk Strait between Sri Lanka and India). The shortest arrival time (21 min) occurs at Port Blair, which is located on the archipelago that divides the Andaman Sea from the Bay of Bengal. Tide gauges to the NE and SE of the Andaman Islands did not record the tsunami [*Oldham*, 1884].

[27] Records from two of the gauges were of inadequate quality to determine precise arrival times or waveform details, and were ignored. The ocean tidal signal was removed from the six remaining clear tsunami records by summing the phase and amplitude data of 37 tidal harmonics calculated for each location and subtracting the resulting time series from the digitized tide gauge records. Because the earthquake occurred on the last day of the 1881 we used the mean amplitudes and phases listed for 1881 and 1882 by *Eccles* [1901]. This revealed one possible error in the recording of the data. An apparent 80 mm subsidence of the Port Blair stilling well relative to sea level during the recording. Because permanent uplift of Port Blair did not occur (Figure 3) we attribute the jump to the tear in the paper that may have shifted it on the drum, or to a jump in the engagement of the sprocket holes in the copper band that linked the drum to the float. The sprocket hole spacing was "about 2.5 inches" [*Eccles*, 1901] so that a sprocket shift alone (63.5 mm) would be inadequate to explain the discrepancy. The mean absolute height of sea level relative to the tide gauge trace was measured regularly [*Eccles*, 1901] so that we may conclude that no significant permanent uplift nor subsidence occurred at Port Blair as a result of the 1881 earthquake.

[28] The Port Blair data are incomplete because the pen periodically ran off the edge of the paper on the drum after the second hour of the event, and because the operator raised the pen to prevent it from damaging the chart [*Walker*, 1883]. Recording recommences after a gap of three hours.

[29] The published data have a duration of 36 hours at each tide gauge and the several hours of data prior to the tsunami permit noise levels to be assessed. Inspection of these records and additional data published by *Eccles* [1901] reveal variable quality of the data recording. For example, short-period seiches are evident in the Negapatam record prior to the arrival of the tsunami (Figure 4). In contrast, the Madras tide gauge data appear deficient in short period waves suggestive of excessive hydraulic filtering probably caused by partial blockage of the entry hole. The tsunami data with tides removed show that the pen and paper recording mechanism of the tide gauges resulted in data that exhibited the effects of friction. These effects introduce additional and unknown phase delays in the tsunami data, and tend to clip peak wave excursions.

6. Localization of the Source Area of the 31 December 1881 Earthquake From the Timing of Tsunami Waves

[30] From the estimated travel time for each tsunami wave (Table 1) and from a knowledge of the precise bathymetry of the Bay of Bengal it is possible to synthesize a series of wave fronts emanating from each tide gauge that intersect at the 1881 source area. The wave front, or ray path, can be draw from each tide gauge backward to the source employing inverse refraction diagrams [*Miyabe*, 1934; *Hatori*, 1969; *Abe*, 1973; *Woods and Okal*, 1987;

Satake, 1988]. In this case, wave fronts were computed by propagating synthetic tsunamis from each tide gauge throughout the Bay of Bengal. A truncated Gauss function (1) was used as an initial condition for these synthetic tsunamis:

$$\eta(r) = \exp(-r^2/b^2); \quad |r| \le 50 \text{ km}$$
$$\eta(r) = 0; \quad |r| > 50 \text{ km}. \tag{1}$$

In equation (1), $b = 22.2$ km, r represents the radial distance from the tide gauge, being η the elevation of the water surface at the initial time. The propagation of the tsunami was simulated by the following linearized shallow water equations [*Pedlosky*, 1979]:

$$\frac{\partial \eta}{\partial t} + \nabla \cdot \mathrm{M} = 0$$
$$\frac{\partial \mathrm{M}}{\partial t} + gh\nabla\eta = 0, \tag{2}$$

where t is time, η is the vertical displacement of the water surface above the still water level (the equipotential surface), h is the ocean depth, M is the horizontal depth-averaged volume flux vector, and g is the gravitational acceleration.

[31] Equations (2) were solved in a set of spherical coordinates using the finite difference method with a staggered leapfrog scheme [*Goto et al.*, 1997]. In the computations the time step was set to 5 s, and the grid spacing to 2 minutes. The bathymetry was interpolated from ETOPO-2 data [*Smith and Sandwell*, 1997]. The propagation time (τ), from each tide gauge to the edge of the initial condition $\eta(50 \text{ km}) = 0.006$ m, was computed from equation (3) along the path (S) described by Snell's law:

$$\tau = \int_S \frac{dS}{\sqrt{gh(S)}}. \tag{3}$$

A tsunami travel time matrix for each tide gauge was obtained on the numerical grid based on the identification of the tsunami wave front at every time step in the numerical model. The time τ was integrated in the travel time matrix.

[32] The preliminary source area (Figure 5) is localized 120 km south of Port Blair between the Andaman trench and Car Nicobar island, in the region of the minimum averaged time square error (the region where the leading wave of the back-propagated waves intersects). The matrix of averaged time square error was computed employing the least squares approach [*Gjevik et al.*, 1997], where each position in space is treated as a possible point source for the tsunami and the averaged travel time square error is calculated for all station data from the corresponding travel time. The error value at the source (minimum value of 3 min) is due both to the instrumental error and to the finite extension of the real source. Figure 5 shows contours of the square root of the averaged time-squared error considering only the travel time from 5 tide gauges on the west side of the Bay of Bengal. Port Blair was not considered here in order to provide an independent analysis due to its evident proximity with the source. Note that this location is independent from, and consistent with, the preliminary location estimates based on the seismic surface wave/tsunami travel time above.

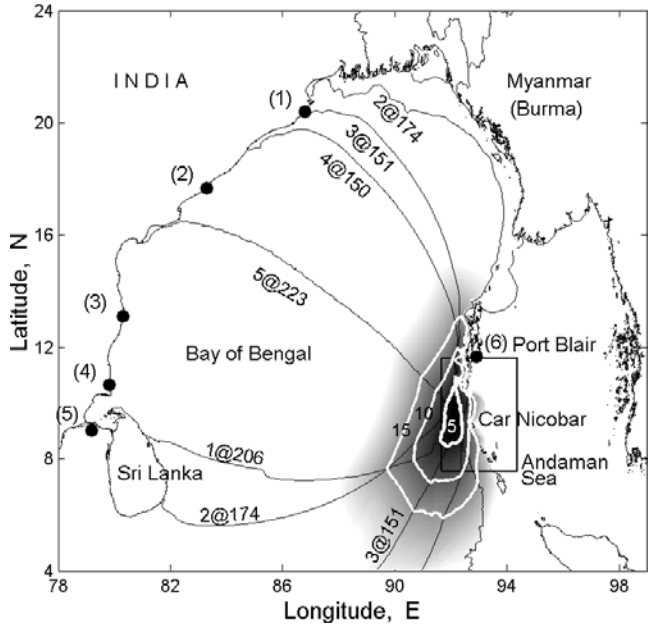

Figure 5. Preliminary location of the 1881 rupture area using the least squares approach [*Gjevik et al.*, 1997]. White contours with labels 5, 10, and 15 on the shading area indicate the square root of the averaged travel time-squared error in min. Backward wave fronts from each tide gauge are also illustrated. The label 3@151, for example, identifies the location of a wave front propagating from gauge 3 after 151 min. As a reference, the west side of the rectangle that contains the source area is localized on the Andaman trench.

7. Test of the Timing of Bay of Bengal Tide Gauges and the Accuracy of Bathymetry Used in the Study

[33] An indirect test of the timing accuracy of the tide gauges is available in the records of the Krakatoa tsunami that was recorded in the Bay of Bengal 2 years after the 1881 earthquake [*Warton and Evans*, 1888]. Knowing the location and time of the Krakatoa eruption we calculated the relative time of arrival of the tsunami at Madras and Negapatam. The synthetic first wave arrival arrives at these two gauges within 1 min of their observed arrival time.

[34] The test confirms our estimates of timing accuracy developed in an earlier section, but has the benefit of confirming the utility of the published bathymetry to estimate tsunami travel times for the 1881 earthquake. Although the test is consistent with Survey of India claims that absolute and relative timing of tide gauges was within 1 min in 1881, clearly, this test does not require it.

8. Inversion of the Port Blair Data to Constrain the Size and Location of the Rupture Zone

[35] The tsunami recorded at Port Blair is the closest to the earthquake and of the six usable tsunami records possess the largest signal-to-noise ratio. We therefore explored the

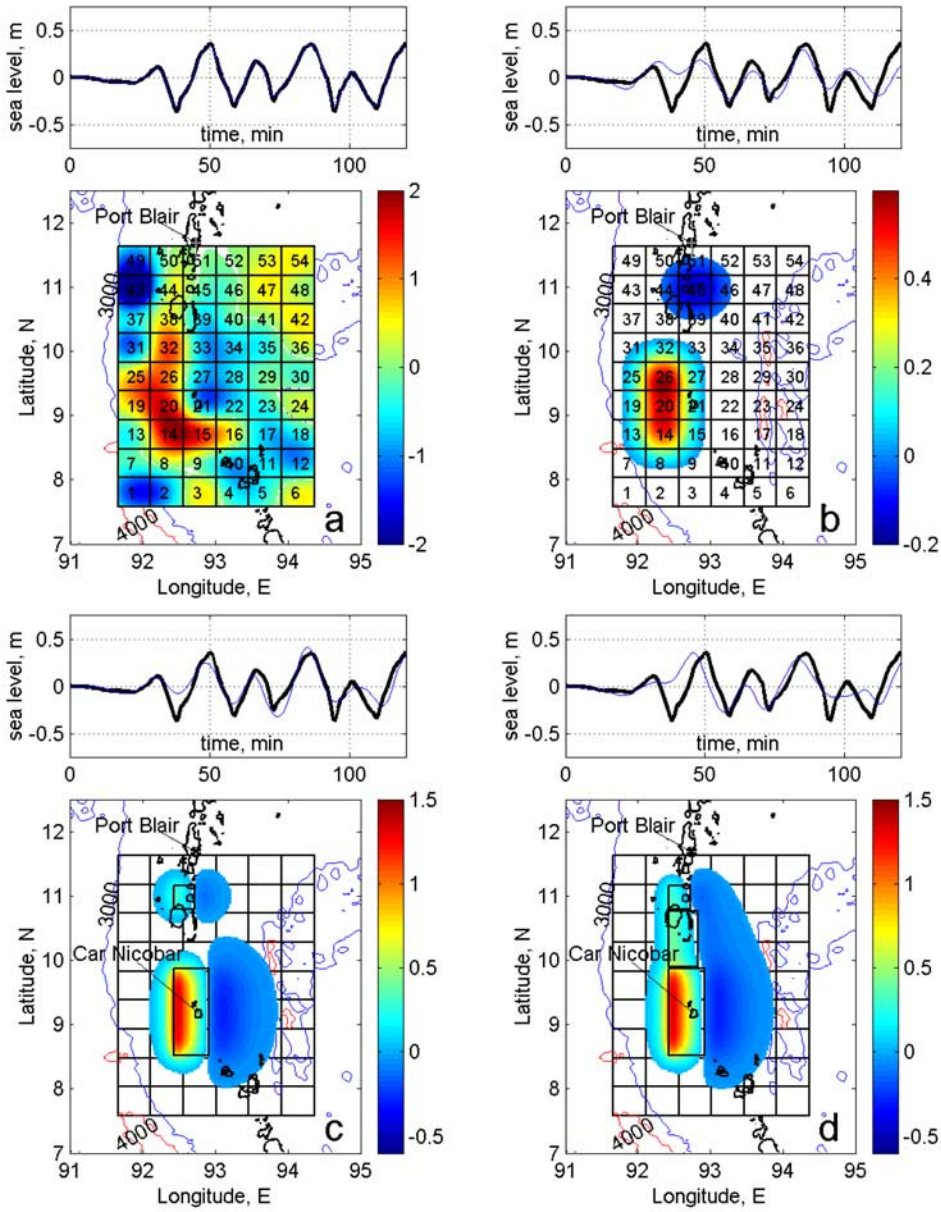

Figure 6. (top) Comparison of the observed (black, thick line) and synthetic (thin, blue line) tsunami at Port Blair. (bottom) Vertical seafloor displacements, color scale in meters. (a) A perfect fit to the data is obtained by allowing 54 Green's functions for the inversion. Each of the numbered areas acts as a rectangular piston that moves at the time of the earthquake. (b) Pistons 14, 20, 26, and 45 allowed to move in the inversion. (c and d) Forward modeling of the tsunami generated by realistic subseafloor dislocations. Rectangles indicate the surface projection of the fault planes. Contours with labels 3000 and 4000 indicate isobaths with the depth values in meters.

possibility of using these data to constrain the precise location of the rupture zone using a minimum norm inversion [*Satake*, 1987]. The method adopted proceeds as follows.

[36] The waveform generated at Port Blair may be considered the linear sum of a series of waves generated by a grid of vertical pistons on the ocean floor that moved individually and synchronously at the time of the earthquake. In Figure 6a we allow 54 such "pistons" (square areas of seafloor each measuring 50 km × 50 km) to move in order to exactly reproduce the Port Blair tsunami (the rectangle that contains the 54 "pistons" in Figure 6a, corresponds to the rectangle indicated in Figure 5 as a reference). The result of this inversion contains no physics of the earthquake source, it merely maps the instantaneous shape of the seafloor needed to reproduce exactly the six crests of the Port Blair tsunami record in the 2 hours following the earthquake. Despite the absence of geophysical constraints, the general features of this inversion are consistent with the findings of backward wave fronts

described above: a coherent region of uplift west of Car Nicobar between 8.5°N and 10.5°N (pistons 14, 20, 26, and 32), with regions of subsidence to the east and west. We tested a finer mesh of pistons and as expected, we can reproduce the observed waveform with arbitrary, nonunique complexity of seafloor motions.

[37] Local regions of pronounced subsidence indicated in Figure 6a (e.g., pistons 43 and 49) could be caused by submarine slumps triggered by the earthquake. This possibility, however, is excluded by the data from tide gauges on the Indian mainland, which are particularly sensitive to the initial geometry in the epicentral region. Besides, tsunami waveforms induced by the movement of pistons southwest of Port Blair (e.g., pistons 43, 44, 49, and 50) are not well constrained by the data and may produce spurious results due to the circumstance that the belt of islands and shoals form a barrier to waves from an origin near the west side of Port Blair. Notice that the movements of individual pistons produce a seafloor deformation that is tapered on neighboring blocks i.e. the uplift (or subsidence) is a smoothed box function for which its one-dimensional wave number spectrum is a cubic sinc function $(k^{-1}\sin k)^3$ that contains only wavelengths greater than the box size (50 km = 20 grid points). This is a desirable property in the numerical model, ensuring that each tsunami wavelength is characterized by at least 20 grid points [*Shuto et al.*, 1986].

[38] Our next few inversion models examined the sensitivity of the tsunami waveform to allowing different combinations of ''pistons'' to move. In these models we imposed the constraint that during the earthquake only a limited part of the seafloor was associated with active deformation (an area constraint), and that subsurface faulting occurred within 100 km of Port Blair (a geometric constraint), in order to reproduce the arrival of the smooth recessional wave that is observed in the record of Port Blair (Figure 4) immediately after the ''earthquake vibrations''. A further constraint is that the resulting seafloor deformation field should be homogeneous and ''smooth,'' a condition imposed by our prejudice that the causal faults slipped with simple geometry.

[39] In the first of these limited area deformation models we confined seafloor motion to pistons 14, 20, and 26 to test whether our geometric constraint was valid. Deformation in these regions alone was unable to reproduce the timing of the Port Blair wave train. However, by allowing piston 45 near Port Blair to move in addition to pistons 14, 20, and 26 we obtained a reasonable fit to the data (Figure 6b). This experiment provided evidence that a northern area of pronounced rupture is necessary to explain the observed tsunami.

[40] We next tested the sensitivity of the solution to the east-west location of the southern rupture, holding the northern rupture fixed (piston 45). In this numerical experiment, seafloor motions were confined to pistons 15, 21, 27, and 45, which yields a reasonable fit to the tsunami at Port Blair but is generated by a physically implausible seafloor deformation field, which we reject. The result of this test suggests that the southern rupture zone must lie west of 92.5°E.

[41] Guided by the rupture location and geometry, and by the amount of sea surface deformation resulting from the inversion, we modeled the tsunami assuming a thrust event for the earthquake on both the southern and northern segments. Thus in Figure 6c we no longer consider seafloor deformation to be caused by a series of unnatural pistons, but by a realistic subseafloor dislocation using the dislocation model of *Mansinha and Smylie* [1971]. The dislocation for the northern segment (reverse slip of 0.9 m) was simulated by a fault plane (50 km × 40 km) dipping 15°E at the depth of 15 km (these rupture parameters are necessary to reproduce the subsidence indicated by piston 45 in Figure 6b). The uplift produced by this dislocation model is southwest of Port Blair in the region where the belt of islands form a barrier to waves toward Port Blair. Therefore the magnitude of the slip of the northern segment is constrained mainly by the region of subsidence. The dislocation for the southern segment (the main rupture) was simulated by a fault plane (150 km × 60 km; reverse slip of 2.7 m) dipping 25° east at the depth of 15 km. This forward modeling of the tsunami yields an acceptable fit to the tsunami waveform and provides us with a starting geometry for subsequent inversion models that incorporate subsurface slip information for the main rupture. We recognize that the above preferred double rupture is somewhat unusual in that it requires two slip patches with no detectable intervening slip. However, forward modeling of the tsunami allowing reverse slip in the region between the two faults does not reproduce adequately the observed wave train at Port Blair. Models with significant slip in this intervening region predict a wave crest arriving at Port Blair at the time of the observed first trough. Figure 6d illustrates the minor misfit at Port Blair attending 1.0 m of reverse slip between the two faults. We note that bimodal or complex slip distributions are by no means atypical of realistic models for earthquake slip. A recent example is the 1995 $M_w = 8.0$ Jalisco earthquake in Mexico [*Melbourne et al.*, 1997].

[42] The tsunami waveforms generated on the mainland coast by the rupture geometry shown in Figure 6c are illustrated in Figure 7. NE of Port Blair, in the vicinity of Rangoon and Moulmein, the height of corresponding tsunami is <2 cm, which agrees the reports of no observed tsunami in that region.

[43] A grid spacing of 81 s was used to specify bathymetry for the whole region, whereas a high-resolution grid of 3 s was used to describe the bathymetry near the coastal areas. The high-resolution bathymetry for the shallow coastal areas was obtained from navigational charts [*Defense Mapping Agency*, 1978–1994].

9. Grid Search to Determine Rupture Parameters Best Fit by the Port Blair Tsunami

[44] In this section we examine the range of acceptable rupture parameters that can be constrained from the Port Blair tsunami. In our search for a unique focal mechanism solution for the 1881 earthquake we computed the equation

$$A_j(t)x_j = b(t),$$

where $A_j(t)$ is the Green's function describing the tsunami generated at Port Blair by movement of the fault, x_j represents the amplitude of slip on the fault, and $b(t)$ is the 125 continuous minutes of observed tsunami record at Port Blair sampled at 1 min intervals.

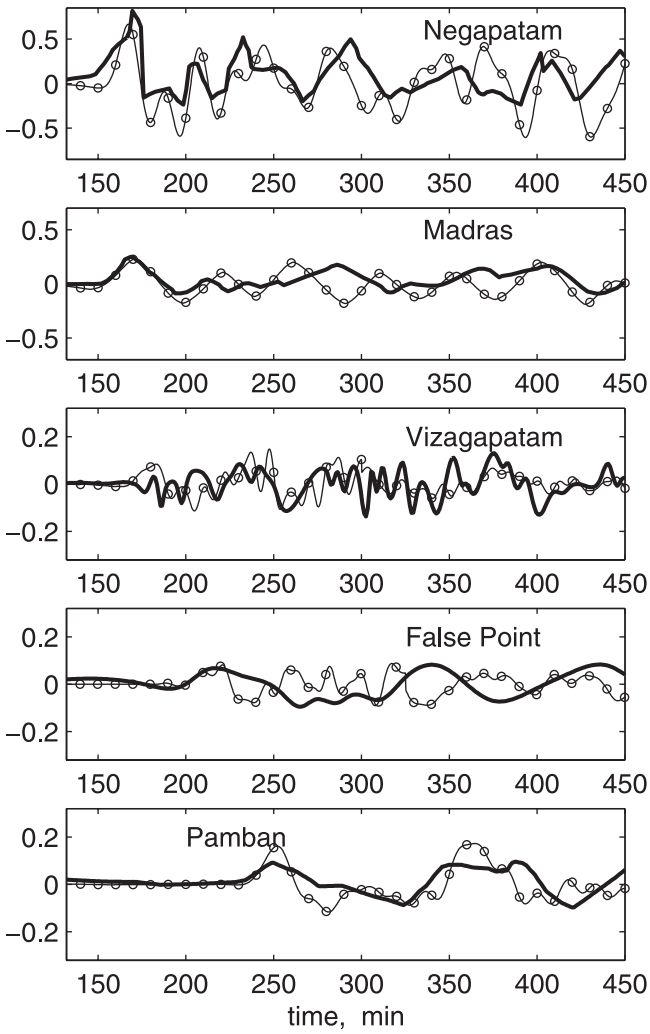

Figure 7. Comparison of the observed (thick line) and synthetic (line with circles at time steps of 10 min) tsunami on the west coast of the Bay of Bengal. The synthetic tsunami is simulated assuming the dislocation model shown in Figure 6c. The origin of the time axis is defined as the origin time of the earthquake. Vertical axis in meters.

[45] We hold the slip of the northern segment constant (0.9 m of slip as above) and examine the best fitting geometric parameters for the southern segment, assuming uniform slip on a buried dislocation. As a quantitative measure of the success of the computation in emulating the observed tsunami waveform we calculated the square root of the mean value of the squares of the residuals between the observed and synthetic tsunamis for each minute in the record. This value divided by the sum of the squares of the estimated uncertainty in the data (11.2 mm for each data point) yields a measure of the acceptability of the solution, sigma. Values of less than unity, one sigma, are considered acceptable. In practice, our estimate of uncertainty of 11.2 mm in the sea level data may be optimistic since it is determined only from estimates of the precision of the tide gauge and does not include oceanic noise. A series of plots illustrate the trade-off in east west location versus depth, width and dip. The most acceptable combinations of these parameters are shown in Figure 8.

[46] From these figures we conclude that the favored location for the 1881 rupture does not differ from the one shown in Figure 6c. The southern lower left edge of the rupture is inferred to be at coordinate 8.52°N, 92.43°E. The length and strike are 150 ± l0 km and 0° ± 10°, the dip and downdip length are 20° ± 5° (dipping east), and 60 ± 10 km, respectively. The depth of the shallow edge of the inferred rupture is estimated to be ~15 km. The mean slip is 270 ± 30 cm for the southern segment, and 90 cm for the northern segment. The rake of the southern and northern segments was assumed constant at 90° (pure reverse faulting consistent with the simple sea surface deformation indicated by previous the inversion). Finally, we search for an area constraint of the northern segment by varying only its length and width at steps of 5 km and holding fixed the best fit parameters of the southern rupture. A well-defined region of minimum sigma values was found for a length of 40 ± 5 km and width of 35 ± 5 km. The geometric parameters of both segments (Table 2) combined represent a $M_w = 7.9 \pm 0.1$ earthquake with 95% of the geometric moment in the main southern rupture. The smaller, northern rupture alone represents a $M_w = 7.0 \pm 0.1$ event.

10. Tsunami Run-Up on Car Nicobar

[47] Our location and depth for the main 1881 rupture places it close to the India/Sunda plate boundary beneath, and to the west of, the island of Car Nicobar. It is from this island that the only reports of possible liquefaction and inferred high intensity shaking in 1881 were recorded

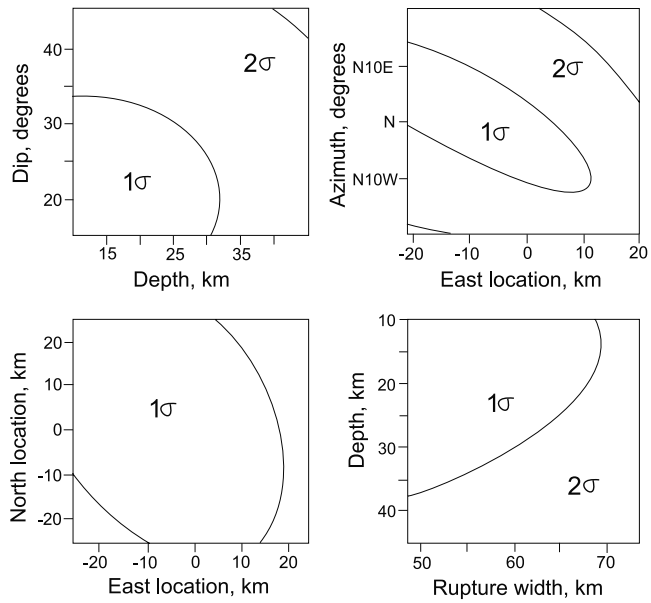

Figure 8. Parameter sensitivity estimates from forward models of the inferred location of the 1881 main shock. In each panel, seven of the nine parameters needed to constrain the elastic dislocation geometry are held constant, and the trade-off in solution space is examined for the parameters indicated.

Table 2. Estimated Rupture Parameters of the 31 December 1881 (M 7.9) Car Nicobar Earthquake[a]

	SW Corner	Length, km	Width, km	Depth, km	Dip, deg	Slip, m	Strike Azimuth, deg	M_0, dyn cm	M_w ±0.1
Southern segment (main rupture)	8.52°N, 92.43°E	150 ± 10	60 ± 10	15	20 ± 5	2.7 ± 0.3	360 ± 10	7.3×10^{27}	7.9
Northern segment	10.75°N, 92.43°E	40 ± 5	35 ± 5	15	15	0.9 ± 0.2	360	3.8×10^{26}	7.0

[a]Rake of 90° (reverse faulting) is assumed for both rupture areas. Moment estimates assume a rigidity modulus of 3×10^{11} dyn cm. M_w estimate uses the relationship: $M_w = 2/3 \log_{10} M_0 - 10.7$ [*Hanks and Kanamori*, 1979].

[*Rogers*, 1883; *Oldham*, 1884]. The steamship *Commonwealth* was directly above the rupture zone (9.3°N) at the time the crew felt the aftershocks of 1 January 1882.

[48] Much of Car Nicobar (maximum elevation ~87 m) is surfaced by corals that testify its recent emergence [*Tipper*, 1911; *Chandra et al.*, 1999]. Maximum vertical deformation during the 1881 earthquake (~1.5 m), however, is not centered on Car Nicobar, which according to our solution is close to a node in the vertical deformation field (Figure 9). Our estimates of coseismic vertical motion of Car Nicobar during the earthquake vary from uplift of 60 cm to subsidence of a few cm depending on the downdip position and width of the rupture. In contrast to this uncertainty in absolute uplift we can be reasonably confident concerning differential movements: we calculate the island would have been tilted by <30 μrad down to the east during the earthquake corresponding to <50 cm of elevation of the east coast relative to the west coast. Hence uplift of the 12 km wide island would have been more pronounced along its western coast.

[49] The rather precise observation of a 76 cm maximum tsunami run-up on Car Nicobar [*Oldham*, 1884] provides a test of our inferred rupture model since it represents the integrated effect of local vertical uplift of the Car Nicobar shoreline, and the tsunami run-up driven by the submarine offshore deformation field. We assume the reference datum used to measure the pile floors of Car Nicobar dwellings to have been maximum high water on the island, but the datum may have been mean high water (30 cm lower). From the Port Blair record we infer this to be mean sea level +1.14 m or +0.84 m, respectively. The tsunami arrived at a time where the tide was roughly 20 cm below high water that day, and the tide dropped roughly 60 cm in the following two hours. We calculate the high tide that day was 0.86 m above mean sea level, i.e., the tsunami initiated when sea level was 0.66 m above mean sea level or 48 cm below maximum high water level. Hence to flood the floor of a pile-supported dwelling at a height of 75 cm above maximum high water the tsunami would have to exceed 75 + 48 cm = 123 cm. The run-up of tsunami waves (Figure 10) arriving after the first maximum would all have been lower because of the ebb tide.

[50] We note that this is consistent with a more distant tsunami than with our preferred location. The calculated disagreement is less if we assume that the mean high water level was the datum used to measure the height of dwellings in Car Nicobar. Given the various uncertainties in the run-

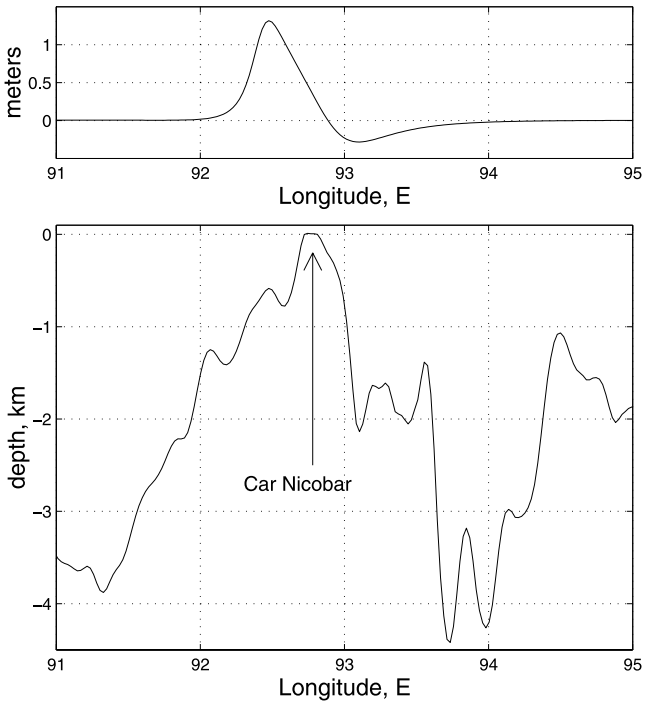

Figure 9. East-west section through Car Nicobar at 9.2°N. (top) Inferred vertical deformation across the island. The eastern shore is close to a node in the deformation field. (bottom) Bathymetric profile across the island.

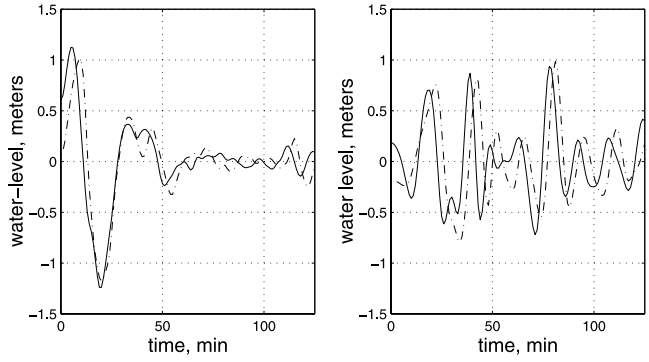

Figure 10. (left) The synthetic 1881 Car Nicobar tsunami for the west coast of Car Nicobar and (right) the corresponding tsunami predicted for the east coast of Car Nicobar. The calculations are relative to mean sea level. Continuous trace predicted from best fit location: dashed trace for rupture 20 km west. In each case the start of the tsunami indicates the uplift of the shore. The best fit location causes uplift of the west and east coasts by 60 cm and 20 cm, respectively, resulting in inferred run-up of 50 cm (west) and 70 cm (east). A more distant westerly rupture location results in uplift of only 10 cm west and subsidence of 20 cm on the east coast, yet the inferred run-up increases to 90 cm and 1.1 m, respectively.

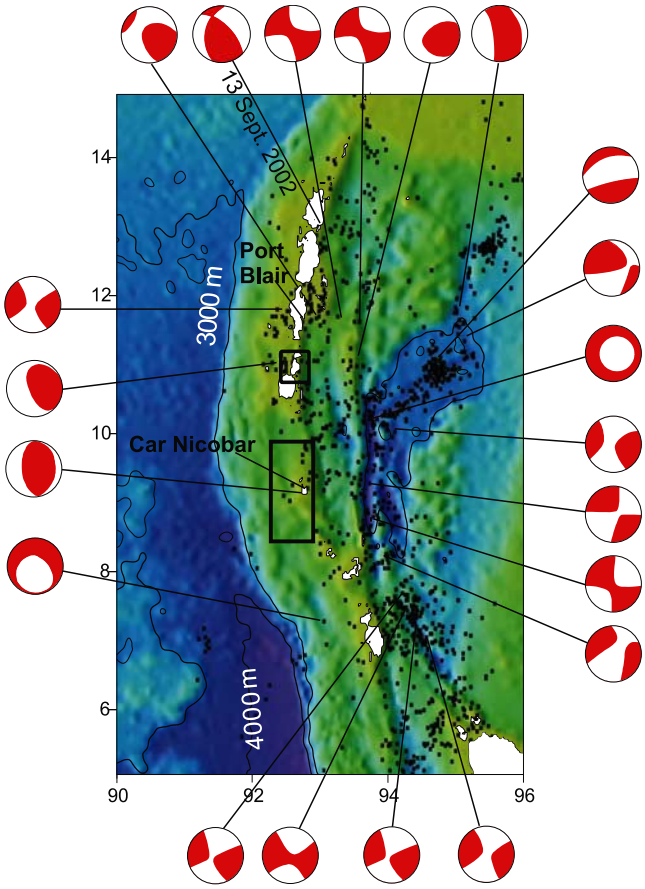

Figure 11. Bathymetry near the Andaman and Nicobar Islands. Rectangles indicate the estimated location of the 31 December 1881 rupture area. Epicenters and focal mechanisms shown are Harvard CMT solutions in the past three decades. The recent 13 September 2002 Andaman earthquake (M_w = 6.5) is also indicated.

up record, it is doubtful that a more precise constraint of the rupture location can be derived from the Car Nicobar tsunami.

11. Discussion: Tectonic Implications of the 1881 Rupture

[51] The forward modeling and inversion methods described above are consistent in that they require two patches to have slipped in the 1881 earthquake: a main rupture 60 km × 150 km elongated north-south that slipped roughly 2.7 m, and an approximately equidimensional 40 km patch that slipped 90 cm. Separating these two is a region of essentially negligible vertical seafloor deformation.

[52] We now speculate on the possible location of the rupture zones using additional constraints from bathymetry, focal mechanisms and recent earthquake depths. Recent focal mechanisms of earthquakes in the region of the main shock (Figure 11) indicate an east-west or N80E thrust component consistent with our rupture estimates, yet a right lateral component of slip might be anticipated from circuit closures of the plate motions in the region. Strike slip, or oblique right-lateral slip, would result in uplift lobes to the NW and SE of the two ruptures, and subsidence to their NE and SW. A series of physically realistic forward models designed to test this possibility failed to identify convincing evidence for oblique slip. Bathymetry near the epicenter, and one focal mechanism near the rupture zone suggest a N5°W strike near the preferred rupture location, which is consistent with our solutions. We therefore conclude that slip was approximately normal to the Andaman transform fault and that partitioning of the strike slip and thrust components of oblique plate boundary convergence prevails here, as it does on the Indonesian arc to the south and southeast [*McCaffrey*, 1994, 1996; *Baroux et al.*, 1998]. A section through the Andaman Islands (see Figure 2) using well-located depths [*Engdahl et al.*, 1998] indicates that the top of the Benioff zone lies between 15 and 40 km in a region close to our inferred source region. The simplest explanation for the 1881 rupture is thus that it represents a plate boundary thrust event.

[53] Although the secondary rupture area north of the main rupture represents ≈28% of the total rupture area it represents <10% of the moment release. The region of negligible slip separating the two ruptures lies directly in line with this region of accretionary tectonics raising the possibility that physical conditions on the fault zone may be influenced by the proximity of the spreading center. North of the Sumatra fault, partitioning between thrust and strike slip displacements effectively ceases. We suspect that the northern rupture may have included an oblique slip component consistent with the observed rotation in the principal axes of focal mechanisms of earthquakes between Car Nicobar and the northern Andamans (Figure 11). Our models are unable to distinguish the relative contributions of thrust and strike slip for this secondary rupture.

[54] An alternative explanation for the sea disturbance north of the main rupture was also explored, the possibility that it was caused by a submarine slump. The subsidence of the northern rupture occurs east of Little Andaman Island where a steep bathymetric slope is mapped in the seafloor, and where a submarine slide could have been triggered by the 1881 main rupture. We found, however, that a submarine slump would not fit the Port Blair tsunami unless it were fed by a considerable subaerial volume from the eastern coastline of the islands. Thus the bipolar signature of a submarine slump is inconsistent with the tsunami record, which requires a broad uplift of the seafloor east of the islands. This broad area of uplift could have been driven without a corresponding region of subsidence only by allowing a thin veneer (e.g., 10 cm thick by at least 30 km × 30 km in area) of submarine sediments to slide eastward, supplemented by subaerial material. Although *Tipper* [1911] suggests that coastal slides may be common throughout the Andaman Islands, the aspect ratio of the slide, and the volume of coastal material required would have substantially have altered the coastline for which there is no evidence.

[55] In contrast to our uncertainties concerning the mechanism of the northern rupture, the slip parameters, location, and tectonic setting of the main rupture are well constrained and are presumably representative of a typical plate boundary rupture in the region. Direct measurements of the full convergence rate between the Sunda Plate and the Indian Plate are currently unavailable although a minimum con-

vergence rate of 15 mm/yr is available from the GPS observation between Port Blair and Bangalore [*Paul et al.*, 2001]. Port Blair lies close to the deforming plate boundary, and plate circuit closure vectors suggest that the convergence rate could be as high as much as 50% higher. If we assume a convergence rate of 18 ± 3 mm/yr we may proceed to estimate a recurrence time for 1881-like events. Slip in the earthquake is calculated to have been 2.7 ± 0.3 m. Were the full convergence rate applied to the rupture zone, elastic strain to drive the next earthquake could be replenished in as little as 240/2.1 = 114 years indicating that a recurrence of the earthquake is imminent. Alternatively, assuming a 3-m mean rupture and the minimum convergence rate yields a significantly longer renewal time of 300/1.5 = 200 years suggesting that the Car Nicobar rupture is barely 60% through an earthquake cycle.

[56] In practice, the displacement loading rate applied to the rupture zone is not the full convergence rate because slip at the plate boundary is partitioned between strike slip on the Sumatra Fault and thrust faulting that we infer to be largely arc normal at the latitude of Car Nicobar. This would reduce the convergence rate by perhaps as much as 30%, extending the recurrence time accordingly. One difficulty in quantifying this precisely is the uncertainty attending the interpretation of the Port Blair GPS vector, which may be sampling an aseismically partitioned convergence rate.

[57] Our study suggests that significant uplift of Car Nicobar Island occurred during the earthquake. It is possible that other coral islands (e.g., the Sentinel Islands) in the archipelago have also been uplifted in historic earthquakes. Hence a history of historic earthquakes may exist in the region interred in the growth rings of corals and marine terraces. Paleogeodetic methods have currently proved successful in revealing the cycle of earthquakes in the Indonesian region [*Zachariasen et al.*, 2000] that no doubt can be applied to the Nicobar and Andaman islands. There is thus room for optimism in believing that the historic record of 1881-like events may be extended by many centuries, and that a sequence of great earthquake rupture zones and recurrence intervals may be developed for India's submarine eastern plate boundary.

12. Conclusions

[58] The 1881earthquake is inferred to have occurred on the upper surface of the Indian Plate beneath Car Nicobar, between the Nicobar Islands and the Andaman Islands. The rupture area of 150 × 60 km^2 with a mean slip of 2.7 m, corresponds to a magnitude $M_w = 7.9 \pm 0.1$ event. The strike and dip of the earthquake are (0 ± 10°N and 20 ± 5°E), starting at a depth of 15–20 km, are consistent with a local bathymetric trend of N355°E and with the upper surface of the plate as defined by well-located microearthquakes and by the focal mechanisms of moderate earthquakes. The disturbance of the seafloor requires two slip patches with negligible intervening slip in an area that corresponds geographically to the westward extension of the Andaman Spreading zone.

[59] The 31 December 1881 Andaman Sea earthquake is probably the earliest earthquake for which the geometry of its rupture zone and its slip distribution has been inferred from teleseismic instrumental records. Constraints of the mechanism of the 1700 Cascadia earthquake have been undertaken using tsunami run-up data from Japan [*Satake et al.*, 1996], and although these provide a lower bound of the moment release, they do not permit the numerical detail imposed by the 1881 tide gauge array. The 1881 event predates the first known teleseismic recording of an earthquake by more than 8 years [*Von Rebeur-Paschwitz*, 1889] and occurs more than two decades before the first global network of seismometers was of sufficient density to locate offshore earthquakes [*Dewey and Byerly*, 1969]. Although precise geodesy has revolutionized the estimation of fault rupture on land, it is presently unable to quantify the geometry and slip of offshore submarine ruptures. The precision with which we have been able to locate the rupture, its area and its slip parameters, is thus unique for its time and location.

[60] We find no evidence for strike-slip motion during the earthquake, which is consistent with recent focal mechanism solutions in the region that suggest that slip partitioning of the convergent and strike-slip components of oblique plate motion prevails. The recurrence time for earthquakes similar to the 1881 Car Nicobar earthquake appears to be 157 ± 43 years, although slip partitioning may result in the recurrence interval being extended by as much as 30%.

[61] We anticipate that the inferred uplift and tilt of Car Nicobar Island during the 1881 earthquake will be recorded in the shallow water coral growth ring history near the island. The examination of these corals both provides a test of the findings presented in this article, and opens the possibility that a several century history of great earthquakes may be available in the region.

Appendix A

[62] The names of the following tide gauge locations have changed since 1881: Madras in now Chennai, Calcutta is Kolkata, Negapatam is Nagapattinam, and Vizapatam is Vishakhapatnam. Port Blair, False Point, Dublat, Pamban and Diamond Harbour remain unchanged.

[63] The earthquake was reported in the press and in Government Reports in 1882. It was felt on the west coast of India [*Logan*, 1887] and may have been felt in the sedimentary basin of Kathmandu. The tsunami data were described in the Annual report of the Survey of India 1881 by *Rogers* [1883] and *Walker* [1883] and repeated in the *Proceedings of the Asiatic Society of Bengal* (1883) and in *Nature* in 1884. Extracts from Oldham's and Walker's accounts are reproduced below. The discussion sections concerning the 1881 epicentral location estimates in Oldham's and Rogers' accounts are omitted.

A1. *Oldham* [1884]

[64] "On the morning of the 31 December 1881 a severe earthquake was felt over a large portion of the Indian Peninsula and Bengal, affecting also the Burmese coast and causing much damage in the Andaman and Nicobar islands. A considerable amount of material, comprising newspaper extracts, official reports and private letters, having been placed at my disposal, I propose giving a brief notice of the more important features of the shock.

[65] In Bengal it was felt as far as Chunar, Gaya and Hazaribagh; Akra in the 24 Parganas, was shaken; and at

Akyab it was followed by the eruption of a mud volcano at Ramri (Records Geological Survey of India, 15, 141). There is no record of it having been felt at Rangoon or Moulmein [in a footnote Oldham states that *Walker* [1884] claims incorrectly that it was felt at both Rangoon and Moulmein]; at Tenasserim (12.1N, 99.1E) it is doubtful, though it was felt in the Mergui archipelago; to the south is reported as having been 'severe' at Acheen in Sumatra, and at 3°54′N, 91°21′E it was felt by the ship *Mount Stuart*; at Oortacamund it is recorded, as also at Calicut: thus the area over which it was felt measures about 1,600 miles from north to south and 1,500 miles from east to west, or 2,000,000 square miles in all.

[66] Such briefly is the summary of the information contained in the daily papers, and as no observation of scientific value is recorded in them which has not been placed at my disposal in another form, I shall refrain from repeating the vague, when not misleading, statements of the time and nature of the shock which were so given to the world (I may however, mention one letter by Mr. W.G. Simmons of Calcutta published in the Indian Daily news. He seems to have been at some trouble to collect information, and I have to thank him for liberally placing it at my disposal).

[67] There is, however, one published notice, which contains much valuable information. I refer to the note by General Walker, and Major M. W. Rogers, R.E. (originally published in the Annual Report of the Trigonometrical Survey, and reprinted in the Proc. Asiatic Soc. Bengal, March 1883, p.60) on the records left by the earthquake, and its consequent sea wave on the tide gauges fixed along the shores of the Bay of Bengal, illustrated by reductions from the original records and a chart of the Bay of Bengal, on which Major Rogers has marked what he considers to be the focus of the disturbance. For the benefit of those who may not have access to the original, I subjoin a short abstract of the information contained.

[68] At Calcutta the time of arrival of the earthquake was noted by Mr. James Murray, who writes, in reply to my inquiries, that he was reading in an upstairs room when feeling the shock he immediately ran downstairs and marked on the glass of his standard regulating clock, the exact position of the second hand and then waited to note the time of cessation of motion; afterward he carefully took with a second's watch the time that occupied to do all he done between the moment he first felt the shock and when he made the first mark on the clock, adding this and the error of the clock on that morning, he obtained the times of commencement and cessation as 7:37:45 and 7:42:00 Calcutta Mean time, or 7:55:02 and 7:59:17 Port Blair mean time, respectively. This, I may add, is the only observation of real value made at the time and not automatically recorded that I know of in connection with this shock.

[69] At Madras a clock in the office of the Master Attendant, electronically controlled from the astronomical observatory, was stopped at 07:05:45 local time or 07:55:36 Port Blair mean time.

[70] ''The only published record of [the Kisseraing seismic arrival] observation is that in Major Rogers' note, where he says that ''at Madras. False Point, and Kisseraing the shock was felt at about the same minute – 7:55'' it will be seen that this is rather vague, and a personal application to Major Rogers elicited the fact that the original record had been destroyed, and it was consequently no longer possible to estimate the degree of accuracy of the time record''.

[71] ''Port Blair is the only place where any damage was done to masonry buildings, and it is to be regretted that the damage should be so little instructive as is the case. The infantry barrack, of which I have drawings showing the damage dome, is a long narrow building situated on the crest of a hill, the major axis bearing N20E, while the cross walls bear E20S. The latter were severely crack, while with a single exception not a crack has opened in the longitudinal walls; this might indicate a direction nearly N20E or S20W but is most probably, as will be seen from the sequel, due to their being of less solid construction. As regards the angle of emergence; the former would be indicated by the fact that a chimney shaft 60 feet high was cracked but not overthrown, as it certainly must have been by a severe shock with a moderate angle of emergence.''

[72] ''In the Nicobar extensive damage was done to the cocoanut groves and the huts of the natives, and vents similar to those described in connection with the Cachar earthquake of 1869 were opened in sandy soil. It was noted by Major W. B. Birch that on the margin of the seashore the trees were left standing, while further inland they were overthrown. The sea wave broke on this island and it is recorded that the water penetrated into the houses of the Burmese residents which stood on platforms of less than 2.5 feet high, while those on higher platforms escaped.''

[73] ''The master of the ship Commonwealth reported that he felt three shocks of earthquake on 1 Jan 1882 at 8°20′N, 92°42′E, and that the whole of the Car Nicobar was hidden by smoke.'' This shock was stated in the daily papers to have been felt in Kathmandu in Nepal, but to judge from the more detailed information placed at my disposal, this cannot have been the same shock.''

A2. *Walker* [1883]

[74] ''On the morning of the 31 December 1881 an earthquake occurred in the Bay of Bengal which operated with considerable violence in the vicinity of the Andaman and Nicobar islands, and with more or less violence along the entire length of the west coast of the Bay, from Ceylon to Calcutta, and was also felt, though comparatively slightly, at various points on the east coast. In addition to ordinary shocks produced by the waves of force acting through the ground, the surface of the ocean was greatly disturbed, and waves were formed which continued to roll against the coastlines for several hours after the cessation of the earth waves, which lasted for only a few seconds.

[75] Both the officers in charge of the tidal operations, first Major Hill and afterward Major Rogers, have taken much pain to ascertain all the facts of the primary ''Great Earth wave'' and the subsequent ''Sea Waves''. It so happens, that at the time of the occurrence of the Earth Wave, Major Rogers was measuring angles with one of the great theodolites of the survey of India at a station on the island of Kisseraing (Burma 9°50′N, 98°50′E) below Tenasserim, on the coast of the Bay as a part of the operations which are described in paragraph 34 of the report. He writes that he ''saw the earthquake before feeling it'', as he was at that moment observing a signal – distant 15 miles – which appeared to rise and fall in the field of the telescope. On

looking at the levels on his instrument, he found that they were violently agitated. He immediately recorded the time at which the phenomenon occurred. Subsequently he ascertained that the earthquake had been felt at almost the same moment at False Point and Madras on the opposite coast. Thus then Major Rogers, assuming the great earthquake to have traveled at equal velocity in all directions from the origin or centre of the impulse, considers that the origin must have been situated at some point in the Bay nearly equidistant from Madras, False Point, and Kisseraing, not in the centre of the triangle joining the three places, but more to the south, toward the line joining Port Blair and Negapatam which was probably the line of greatest disturbance, as at those places the sea waves were greatest.

[76] It is remarkable that there should be no indication of any sea wave at either of the tide al stations at Rangoon, Elephant Point, Moulmein or Amherst. This may be due to the circumstance that the belt of islands and shoal which extends from Cape Negrais down to the Island of Sumatra forms a barrier to waves from an origin near the centre of the Bay, the sea waves were propelled with great violence against these islands on all sides and over the surrounding shallows, but they seem to have died away very rapidly in the deep sea beyond. Moreover the earthquake wave must have operated with far greater force toward the west than toward the east of the centre of the impulse; for violent shocks were felt all along the west coast of the Bay, and to a considerable distance inland, whereas on the east coast the shocks were very slight and barely perceptible.

[77] **Acknowledgments.** We thank J. Curray for his helpful review and for providing bathymetric sections in the Andaman region. P. Leverenz for providing access to the valuable Bathymetric Map Collection from Scripps Institution of Oceanography, and numerous colleagues with whom we have discussed aspects of the analysis. We thank K. Satake for his helpful review. R.B. acknowledges support from the National Science Foundation and from a John Simon Guggenheim foundation Fellowship that made this study possible. M.O. acknowledges support from NIED (National Research Institute for Earth Science and Disaster Prevention, Japan).

References

Abe, K., Tsunami and mechanism of great earthquakes, *Phys. Earth Planet. Inter.*, *7*, 143–153, 1973.

Agnew, D. C., Detailed analysis of tide gauge data: A case history, *Mar. Geod.*, *10*, 231–255, 1986.

Agrawal, P. N., A study of the 20 January 1982 earthquake near the Great Nicobar Island, India, *Bull. Seismol. Soc. Am.*, *73*, 1139–1159, 1983.

Banghar, A. R., Seismo-tectonics of the Andaman-Nicobar islands, *Tectonophysics*, *133*, 95–107, 1987.

Baroux, E., J.-P. Avouac, O. Bellier, and M. Sebrier, Slip partitioning and fore arc deformation of the Sunda trench, Indonesia, *Terra Nova*, *10*, 139–144, 1998.

Bilham, R., A sea level recorder for tectonic studies, *Geophys. J. R. Astron. Soc.*, *48*, 307–314, 1977.

Chandra, A., R. K. Saxena, and A. K. Ghosh, Coralline algae from the Kakana Formation (Middle Pliocene) of Car Nicobar Island, India and their implications in biostratigraphy, palaeoenvironment and palaeobathymetry, *Current Sci.*, *76*(11), 1498–1502, 1999.

Curray, J. R., F. J. Emmel, D. G. Moore, R. W. Raitt, M. Henry, and R. Kieckhefer, Tectonics of the Andaman sea and Burma, in *Geological and Geophysical Investigations of Continental Margins*, edited by J. S. Watkins, L. Montadert, and P. Dickerson, *AAPG Mem.*, *29*, 189–198, 1979.

Curray, J. R., F. J. Emmel, D. G. Moore, and R. W. Raitt, Structure, tectonics and geological history of the NE Indian Ocean, in *The Ocean Basins and Margins*, vol. 6. *The Indian Ocean*, edited by A. E. M. Nairn and F. G. Sehli, pp. 399–450, Plenum, New York, 1982.

Dasgupta, and M. Mukhopadhyaya, Seismicity and plate deformation below the Andaman Arc, northeastern Indian Ocean, *Tectonophysics*, *225*, 529–542, 1993.

Dasgupta, S., Seismotectonics and stress distribution in the Andaman Plate, *Mem. Geol. Soc. India*, *23*, 319–334, 1993.

Defense Mapping Agency, Hydrographic/Topographic Center, Navigational charts: 63383, 63260, 63291, 63271, 63324, 63250, Washington, D.C., 1978–1994.

DeMets, C., R. G. Gordon, D. F. Argus, and S. Stein, Current plate motions, *Geophys. J. Int.*, *101*, 425–478, 1990.

DeMets, C., R. G. Gordon, D. F. Argus, and S. Stein, Effect of recent revisions to the geomagnetic reversal time scale on estimate of current plate motions, *Geophys. Res. Lett.*, *21*, 2191–2194, 1994.

Dewey, J., and P. Byerly, The early history of seismometry (to 1900), *Bull. Seismol. Soc. Am.*, *59*, 1, 83–227, 1969.

Eccles, J., Account of the operations of the great trigonometrical survey of India: Details of the tidal observations taken during the period from 1873 to 1892, *Dehra Dun*, *XVI*, Surv. of India, Dehra Dun, 1901.

Eguchi, T., S. Uyeda, and T. Maki, Seismotectonics of the Andaman Sea, *Tectonophysics*, *57*, 35–51, 1979.

Engdahl, E. R., R. D. Van der Hilst, and R. P. Buland, Global teleseismic earthquake relocation with improved travel times and procedures for depth determination, *Bull. Seism. Soc. Amer.*, *88*, 722–743, 1998.

Fitch, T. J., Earthquake mechanisms in the Himalayan, Burmese and Andaman regions and continental tectonics in Asia, *J. Geophys. Res.*, *75*, 2699–2709, 1970.

Gjevik, B. G., G. Pedersen, E. Dybesland, C. B. Harbitz, P. M. A. Miranda, M. A. Baptista, L. Mendes-Victor, P. Heinrich, R. Roche, and M. Guesmia, Modeling tsunamis from earthquake sources near Gorringe Bank southwest of Portugal, *J. Geophys. Res.*, *102*, 27,931–27,949, 1997.

Goto, C., Y. Ogawa, N. Shuto, and F. Imamura, IUGG/IOC TIME Project: Numerical method of tsunami simulation with the leap-frog scheme, *Manuals Guides 35*, 4 parts, Intergovt. Oceanogr. Comm. of UNESCO, Paris, 1997.

Government Report, 1881 annual report on the administration of the Andaman and Nicobar Islands, and the Penal Settlement of Port Blair, Govt. of India, Calcutta, 1882.

Hanks, T. C., and H. Kanamori, A moment magnitude scale, *J. Geophys. Res.*, *84*, 2348–2350, 1979.

Hatori, T., Dimensions and geographical distribution of tsunami sources near Japan, *Bull. Earthquake Res. Inst. Univ. Tokyo*, *47*, 185–214, 1969.

Home Department, Selections from the records of the government of India (Home Department) 25, The Andaman islands with notes on Barren Island, Calcutta, 131 pp., 1859.

Hunter, W. W., J. S. Cotton, R. Burn, and W. S. Meyer, *The Imperial Gazetteer of India*, Clarenden, Oxford, England, 1909.

Jhingran, A. G., A note on the earthquake in the Andaman Islands (26 June 1941), *Rec. Geol. Surv. India*, *82*(2), 300–307, 1953.

Krishnan, R., General report for 1941, *Rec. Geol. Surv. India*, *79*(1), 193–194, 1953.

Kurz, S., Report on the vegetation of the Andamas, 196 pp., Govt. of India, Calcutta, 1868. (Reprinted 1890.)

Logan, W., *The Malabar Manual*, 2 vols., 759 pp., Asian Educ. Serv., New Delhi, 1887. (Reprinted 1995.)

Mansinha, L., and D. E. Smylie, The displacement field of inclined faults, *Bull. Seismol. Soc. Am.*, *61*, 1433–1440, 1971.

Maung, H., Transcurrent movements in the Burma-Andaman Sea region, *Geology*, *15*, 911–912, 1987.

McCaffrey, R., Global variability in subduction thrust zone-forearc systems, *Pure Appl. Geophys.*, *142*, 173–224, 1994.

McCaffrey, R., Slip partitioning at convergent boundaries of SE Asia, in *Tectonic Evolution of Southeast Asia*, edited by R. Hall and D. Blundell, *Geol. Soc. Spec. Publ.*, *106*, 3–18, 1996.

Melbourne, T., I. Carmichael, C. DeMets, K. Hudnut, O. Sanchez, J. Stock, and G. Suraez, The geodetic signature of the *M*8.0 Oct. 9, 1995, Jalisco subduction earthquake, *Geophys. Res. Lett.*, *24*, 715–718, 1997.

Miyabe, N., An investigation of the Sanriku tsunami based on mareogram data, *Bull. Earthquake Res. Inst. Univ. Tokyo*, *1*, suppl., 112–126, 1934.

Murty, T. S., and M. Rafiq, A tentative list of tsunamis in the Marginal Seas of the North Indian Ocean, *Nat. Hazards*, *4*, 81–83, 1991.

Newcomb, K. R., and W. R. McCann, Seismic history and seismotectonics of the Sunda Arc, *J. Geophys. Res.*, *92*, 421–439, 1987.

Oldham, R. D., Note on the earthquake of 31 December 1881, *Rec. Geol. Surv. India*, *17*(2), 47–53, 1884.

Oldham, R. D., Geology of the Andaman Islands with references to the Nicobars, *Rec. Geol. Surv. India*, *18*(3), 135–145, 1885.

Paul, J., et al., The motion and active deformation of India, *Geophys. Res. Lett.*, *28*, 647–651, 2001.

Pedlosky, J., *Geophysical Fluid Dynamics*, 624 pp., Springer-Verlag, New York, 1979.

Rajendran, K., and H. K. Gupta, Seismicity and tectonic stress-field of a part of the Burma-Andaman-Nicobar Arc, *Bull. Seismol. Soc. Am.*, *79*, 989–1005, 1989.

Rogers, R. E., Memorandum on the earthquake of the 31st December 1881 and the great sea-waves resulting therefrom, as shown on the diagrams of the tidal observatories in the Bay of Bengal, in *General Report on the Operations of the Survey of India 1881–1882*, pp. 70–73, Govt. Print. Off., Calcutta, 1883.

Satake, K., Inversion of tsunami waveforms for the estimation of a fault heterogeneity: Method and numerical experiments, *J. Phys. Earth*, *35*, 241–254, 1987.

Satake, K., Effects of bathymetry on tsunami propagation: Application of ray tracing to tsunamis, *Pure Appl. Geophys.*, *126*, 28–35, 1988.

Satake, K., K. Shimazaki, Y. Tsuji, and K. Ueda, Time and size of a giant earthquake in Cascadia inferred from Japanese tsunami records of January 1700, *Nature*, *379*, 246–249, 1996.

Shuto, N., T. Suzuki, K. Hasegawa, and K. Inagaki, A study of numerical technique on the tsunami propagation and run-up, *Sci. Tsunami Hazard*, *4*, 111–124, 1986.

Sinvhal, H., K. N. Khattri, K. Rai, and V. K. Gaur, Neo-tectonics and time-space seismicity of the Andaman-Nicobar region, *Bull. Seismol. Soc. Am.*, *68*, 399–409, 1978.

Smith, W. H. F., and D. T. Sandwell, Global seafloor topography from satellite altimetry and ship depth soundings, *Science*, *227*, 1956–1962, 1997.

Srivastava, H. N., and H. M. Chaudhury, Seismicity and focal mechanism of earthquakes in Andaman islands, *Mausam*, *30*(2), 213–220, 1979.

Tipper, G. H., The geology of the Andaman Islands, *Mem. Geol. Surv. India*, *35*, 4, 1911.

Von Rebeur-Paschwitz, E., The earthquake of Tokio, April 18, 1889, *Nature*, *40*, 294–295, 1889.

Walker, J. T., The earthquake of the 31 December 1881, General report on the operations of the Survey of India 1881–1882, pp. 53–55, Surv. of India, Kolkata, 1883. (Reprinted in proceedings of the Asiatic Society of Bengal, p. 60, March 1883.)

Walker, J. T., Earthquake disturbances of the tides on the coasts of India, *Nature*, *28*, 358–360, 1884.

Wang, Q., et al., Present day crustal deformation in China constrained by Global Positioning measurements, *Science*, *294*, 574–577, 2001.

Warton, W. J. L., and F. J. Evans, On the seismic sea waves caused by the eruption at Krakatoa, August 26th and 27th, 1883—The eruption of Krakatoa and subsequent phenomena, in *Report of the Krakatoa*, edited by G. L. Symonds, *Commun. R. Soc.*, *3*, 89–151, 1888.

Woods, M. T., and E. A. Okal, Effect of variable bathymetry on the amplitude of teleseismic tsunamis: A ray-tracing experiment, *Geophys. Res. Lett.*, *14*, 765–768, 1987.

Zachariasen, J., K. Sieh, F. W. Taylor, and W. S. Hantoro, Modern vertical deformation above the Sumatran subduction zone: Paleogeodetic insights from coral microatolls, *Bull. Seismol. Soc. Am.*, *90*, 897–913, 2000.

R. Bilham, CIRES and Geological Sciences, University of Colorado, Boulder CO 80309, USA. (bilham@colorado.edu)

M. Ortiz, Departamento de Oceanografía, CICESE, Ensenada, Baja California 22860, México. (ortizf@cicese.mx)